

Collective excitations and neutrino-nucleus reactions in relativistic point-coupling models

APCTP, Pohang

Deni Vale, Nils Paar, Tamara Nikšić, Yifei Niu

University of Zagreb, Faculty of Science, Department of Physics

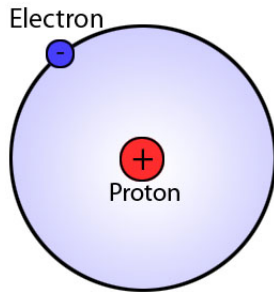
July 5, 2019



QuantiXLie

CENTER OF EXCELLENCE FOR THE THEORY OF QUANTUM AND COMPLEX SYSTEMS AND LIE ALGEBRA REPRESENTATION

Simple system - Hydrogen atom



Simple system - Hydrogen atom

Dirac Hamiltonian for central field:

$$\hat{H} = c\hat{\vec{\alpha}} \cdot \hat{\vec{p}} + \beta m_0 c^2 + V(r) \quad (1)$$

If the field has spherical symmetry, then total angular momentum operator \hat{J} and operator \hat{P} ($\hat{P} = \exp(i\phi)\hat{\beta}\hat{P}_0$, $P_0 : \vec{x} \rightarrow -\vec{x}$) commute with \hat{H} .

We assume solution:

$$\Psi_{njm} = \begin{pmatrix} \psi_{ljm}(\vec{r}, t) \\ \chi_{\bar{l}jm}(\vec{r}, t) \end{pmatrix} \quad (2)$$

Action of parity operator:

$$\hat{P}_0 \psi_{ljm}(\vec{r}, t) = \lambda_f \psi_{ljm}(\vec{r}, t) \quad (3)$$

$$-\hat{P}_0 \chi_{\bar{l}jm}(\vec{r}, t) = -\lambda_g \chi_{\bar{l}jm}(\vec{r}, t) \quad (4)$$

We must have $\lambda_f = -\lambda_g$ in order to have good parity of four-spinor.

Simple system - Hydrogen atom

$$\begin{aligned}\hat{H}\Psi_{jm}(\vec{r}, t) = & -i\hbar \begin{pmatrix} 0 & \hat{\vec{\sigma}} \\ \hat{\vec{\sigma}} & 0 \end{pmatrix} \nabla \Psi_{jm}(\vec{r}, t) + \begin{pmatrix} 1 & 0 \\ 0 & -1 \end{pmatrix} m_0 c^2 \Psi_{jm}(\vec{r}, t) \\ & + V(r) \Psi_{jm}(\vec{r}, t)\end{aligned}\quad (5)$$

Rewritten in terms of bispinors:

$$-i\hbar c \vec{\sigma} \cdot \vec{\nabla} \chi_{ljm} + m_0 c^2 \psi_{ljm} + V(r) \psi_{ljm} = E \psi_{ljm} \quad (6)$$

$$-i\hbar c \vec{\sigma} \cdot \vec{\nabla} \psi_{ljm} - m_0 c^2 \chi_{ljm} + V(r) \chi_{ljm} = E \chi_{ljm} \quad (7)$$

For ψ

$$\psi_{ljm} = R_{nl}(r) \sum_{m_l m_s} C_{1/2 m_s l m_l}^{jm} Y_{lm_l}(\Omega) \chi_{1/2 m_s}(\vec{\sigma}) \quad (8)$$

and similar for χ .

Expansion of bispinors in spherical harmonic oscillator basis:

$$\psi_{nljm} = \sum_n C_n^l f_{nl}(r) \Omega_{ljm}(\hat{\Omega}) \quad (9)$$

$$\chi_{n\bar{l}jm} = \sum_n C_n^{\bar{l}} g_{n\bar{l}}(r) \Omega_{\bar{l}jm}(\hat{\Omega}) \quad (10)$$

Simple system - Hydrogen atom

Matrix elements of Dirac Hamiltonian:

$$A_{fg} = -\hbar c \int_0^\infty dr r^2 f_{n_a l_a}^*(r) \frac{\partial}{\partial r} g_{n_c \bar{l}_a}(r) \quad (11)$$

$$B_{fg} = -\hbar c \int_0^\infty dr r^2 f_{n_a l_a}^*(r) \frac{1-\kappa}{r} g_{n_c \bar{l}_a}(r) \quad (12)$$

$$C_{ff}^{(S)} = \int dr r^2 f_{n_a l_a}^*(r) S(r) f_{n_c l_a}(r) \quad (13)$$

$$C_{ff}^{(V)} = \int dr r^2 f_{n_a l_a}^*(r) V(r) f_{n_c l_a}(r) \quad (14)$$

$$A_{gf} = \hbar c \int_0^\infty dr r^2 g_{n_a \bar{l}_a}^*(r) \frac{\partial}{\partial r} f_{n_c l_a}(r) \quad (15)$$

$$B_{gf} = \hbar c \int_0^\infty dr r^2 g_{n_a \bar{l}_a}^*(r) \frac{1+\kappa}{r} f_{n_c l_a}(r) \quad (16)$$

$$C_{gg}^{(S)} = - \int dr r^2 g_{n_a \bar{l}_a}^*(r) S(r) g_{n_c \bar{l}_a}(r) \quad (17)$$

$$C_{gg}^{(V)} = \int dr r^2 g_{n_a \bar{l}_a}^*(r) V(r) g_{n_c \bar{l}_a}(r) \quad (18)$$

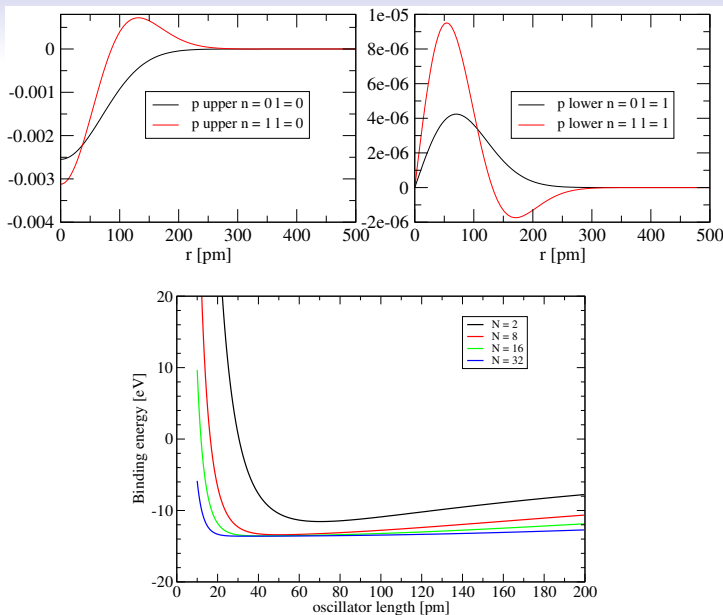
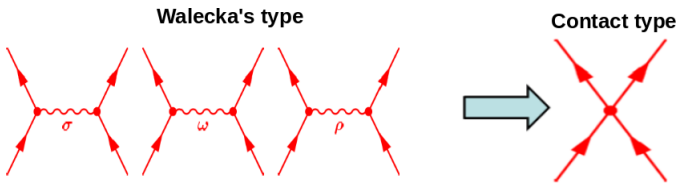


Figure 1: Upper and lower components of spinor $s_{1/2}$. Dependence of binding energy of hydrogen atom on harmonic oscillator length for different numbers of major oscillator shells.

Relativistic nuclear energy density functionals

Two types of nuclear models are usually present in relativistic energy density functionals:

- Walecka's type (nucleons are system of Dirac particles which interacts by exchange of mesons)
- Contact type (point-coupling; where meson propagator is replaced by contact interaction)



In nuclear models of Walecka's type we have meson propagator:

$$\frac{g_m}{-\Delta + m_m^2} \simeq \frac{g_m}{m_m^2} + g_m \frac{\Delta}{m_m^4}, \quad (19)$$

Four-fermion interaction:

$$\begin{aligned} L_{4f} = & -\frac{1}{2}\alpha_S (\bar{\psi}\psi)(\bar{\psi}\psi) - \frac{1}{2}\alpha_V (\bar{\psi}\gamma_\mu\psi)(\bar{\psi}\gamma^\mu\psi) \\ & - \frac{1}{2}\alpha_{TV} (\bar{\psi}\vec{\tau}\gamma_\mu\psi)(\bar{\psi}\vec{\tau}\gamma^\mu\psi), \quad (20) \end{aligned}$$

Derivative terms:

$$\begin{aligned} L_{der} = & -\frac{1}{2}\delta_S \partial_\nu (\bar{\psi}\psi) \partial^\nu (\bar{\psi}\psi) - \frac{1}{2}\delta_V \partial_\nu (\bar{\psi}\gamma_\mu\psi) \partial^\nu (\bar{\psi}\gamma^\mu\psi) \\ & - \frac{1}{2}\delta_{TV} \partial_\nu (\bar{\psi}\vec{\tau}\gamma_\mu\psi) \partial^\nu (\bar{\psi}\vec{\tau}\gamma^\mu\psi), \quad (21) \end{aligned}$$

We can add non-linear terms:

$$L_{hot} = -\frac{1}{3}\beta_S (\bar{\psi}\psi)^3 - \frac{1}{4}\gamma_S (\bar{\psi}\psi)^4, \quad (22)$$

Dirac Lagrangian for free nucleon:

$$L_{free} = \bar{\psi}(i\gamma_\mu\partial^\mu - m)\psi \quad (23)$$

Electromagnetic part:

$$L_{em} = -eA_\mu\bar{\psi}[(1-\tau_3)/2]\gamma^\mu\psi - \frac{1}{4}F_{\mu\nu}F^{\mu\nu} \quad (24)$$

DD-PC1 parametrization

Lagrangian density:

$$\begin{aligned}
 L = & \bar{\psi} (i\gamma_\mu \partial^\mu - m) \psi - \frac{1}{2} \alpha_S (\bar{\psi} \psi) (\bar{\psi} \psi) - \frac{1}{2} \alpha_V (\bar{\psi} \gamma_\mu \psi) \\
 & \times (\bar{\psi} \gamma^\mu \psi) - \frac{1}{2} \alpha_{TV} (\bar{\psi} \vec{\tau} \gamma_\mu \psi) (\bar{\psi} \vec{\tau} \gamma^\mu \psi) \\
 & - \frac{1}{2} \delta_S \partial_\nu (\bar{\psi} \psi) \partial^\nu (\bar{\psi} \psi) - e \bar{\psi} \gamma_\mu A^\mu \frac{1 - \tau_3}{2} \psi. \quad (25)
 \end{aligned}$$

Coupling density dependence in case of DD-PC1 parametrization:

$$f_i [\rho] = a_i + (b_i + c_i x) \exp(-d_i x), \quad (26)$$

Variation of Lagrangian with respect to $\bar{\psi}$ we obtain one-nucleon Dirac equation:

$$[\gamma_\mu (i\partial^\mu - \Sigma^\mu - \Sigma_{rear}^\mu) - (m + \Sigma_S)] \psi = 0, \quad (27)$$

$$\Sigma^\mu = \Sigma_V^\mu + \vec{\tau} \cdot \vec{\Sigma}_{TV}^\mu, \quad (28)$$

$$\Sigma_S = \alpha_S(\rho) \rho_S + \delta_S \Delta \rho_S, \quad (29)$$

$$\Sigma_V^\mu = \alpha_V(\rho) j^\mu + e \frac{1 - \tau_3}{2} A^\mu, \quad (30)$$

$$(31)$$

$$\vec{\Sigma}_{TV}^\mu = \alpha_{TV}(\rho) \vec{j}^\mu, \quad (32)$$

$$\Sigma_{\text{rearr}}^\mu = \frac{1}{2} \frac{j^\mu}{\rho} \left[\frac{\partial \alpha_S(\rho)}{\partial \rho} \rho_S^2 + \frac{\partial \alpha_V(\rho)}{\partial \rho} j_\nu j^\nu + \frac{\partial \alpha_{TV}(\rho)}{\partial \rho} \vec{j}_\nu \vec{j}^\nu \right]. \quad (33)$$

RPA matrix elements can be easily obtained from:

$$V_{abcd} = \frac{\delta h_{ac}}{\delta \rho_{db}} = \frac{\delta^2 E[\rho]}{\delta \rho_{ac} \delta \rho_{bd}}, \quad (34)$$

where

$$h = -i\boldsymbol{\alpha}\nabla + \beta(m + \Sigma) + \beta\gamma_\mu\Sigma^\mu \quad (35)$$

General particle-hole matrix elements

$$\begin{aligned}
 V_{abcd}^{(1)} = & \int d^3 r_1 \int d^3 r_2 \sum_j \bar{\psi}_a(\vec{r}_1) \Gamma_{j\mu}^{(1)} O_\tau^{(1)} \psi_c(\vec{r}_1) D_j(\vec{r}_1, \vec{r}_2) \\
 & \times \bar{\psi}_b(\vec{r}_2) \Gamma_j^{(2)\mu} O_\tau^{(2)} \psi_d(\vec{r}_2) \quad (36)
 \end{aligned}$$

$$\begin{aligned}
 V_{abcd}^{(2)} = & \int d^3 r_1 \int d^3 r_2 \sum_j \bar{\psi}_a(\vec{r}_1) \Gamma_{j\mu}^{(1)} O_\tau^{(1)} \psi_c(\vec{r}_1) \frac{\partial D_j(\vec{r}_1, \vec{r}_2)}{\partial \rho(\vec{r}_1)} \\
 & \times \rho_j^\mu(\vec{r}_2) \bar{\psi}_b(\vec{r}_2) 1^{(2)} \psi_d(\vec{r}_2) \quad (37)
 \end{aligned}$$

$$\begin{aligned}
 V_{abcd}^{(3)} = & 1/2 \int d^3 r_1 \int d^3 r_2 \sum_j \bar{\psi}_a(\vec{r}_1) 1^{(1)} \psi_c(\vec{r}_2) \frac{\partial D_j^2(\vec{r}_1, \vec{r}_2)}{\partial \rho^2(\vec{r}_1)} \\
 & \times \rho_{j\mu}(\vec{r}_1) \rho_j^\mu(\vec{r}_2) \bar{\psi}_b(\vec{r}_2) 1^{(2)} \psi_d(\vec{r}_2) \quad (38)
 \end{aligned}$$

$$\begin{aligned}
 V_{abcd}^{(4)} = & \int d^3 r_1 \int d^3 r_2 \sum_j \bar{\psi}_a(\vec{r}_1) 1^{(1)} \psi_c(\vec{r}_2) \frac{\partial D_j(\vec{r}_1, \vec{r}_2)}{\partial \rho(\vec{r}_1)} \\
 & \times \rho_{j\mu}(\vec{r}_1) \bar{\psi}_b(\vec{r}_1) \Gamma_j^{(2)\mu} O_\tau^{(2)} \psi_d(\vec{r}_2), \quad (39)
 \end{aligned}$$

Separable pairing matrix elements

In 2009 Y. Tian, Z. Y. Ma and P. Ring introduced separable pairing in 1S_0 channel gap equation of symmetric nuclear matter:

$$\Delta(k) = - \int_0^\infty \frac{k'^2 dk'}{2\pi^2} \langle k | V_{sep}^{^1S_0} | k' \rangle \frac{\Delta(k')}{2E(k')}, \quad (40)$$

where

$$\langle k | V_{sep}^{^1S_0} | k' \rangle = - G p(k) p(k'), \quad (41)$$

with Gaussian ansatz

$$p(k) = e^{-a^2 k^2}. \quad (42)$$

These two parameters a and G were fitted to density dependence of the gap at the Fermi surface in nuclear matter. After transformation the separable force from momentum to coordinate space we obtained:

$$V(\vec{r}_1, \vec{r}_2, \vec{r}'_1, \vec{r}'_2) = - G \delta(\vec{R}_1 - \vec{R}_2) P(r) P(r') \frac{1 - \hat{P}^\sigma}{2} \quad (43)$$

with $\vec{r} = 1/\sqrt{2}(\vec{r}_1 - \vec{r}_2)$ and $\vec{R} = 1/\sqrt{2}(\vec{r}_1 + \vec{r}_2)$. Values of $G = 728$ MeV fm 3 and $a_0 = 0.644$ fm

Separable pairing matrix elements

After Fourier transformation:

$$P(r) = \frac{e^{-r^2/(2a^2)}}{(4\pi a^2)^{3/2}} \quad (44)$$

Due to coordinate transformation from laboratory to center of mass and relative coordinates we need to use Talmi-Moschinsky brackets:

$$|n_1 l_1, n_2 l_2; \lambda \mu\rangle = \sum_{NLnl} M_{n_1 l_1 n_2 l_2}^{NLnl} |NL, nl; \lambda \mu\rangle \quad (45)$$

If we work in the basis of spherical harmonic oscillator:

$$I_n = \sqrt{4\pi} \int R_{nl}(r) P(r) r^2 dr = \frac{1}{2^{2/3} \pi^{3/4} b^{3/2}} \frac{(1-\alpha^2)^n}{(1+\alpha^2)^{n+3/2}} \frac{\sqrt{2n+1}}{2^n n!}, \quad (46)$$

the coupled matrix element for $T = 1$ pairing:

$$\begin{aligned} V_{abcd}^{JM} &= G \hat{j}_a \hat{j}_b \hat{j}_c \hat{j}_d (-1)^{l_b + l_d + j_a + j_c} \left\{ \begin{array}{ccc} l_a & j_a & 1/2 \\ j_b & l_b & J \end{array} \right\} \left\{ \begin{array}{ccc} l_c & j_c & 1/2 \\ j_d & l_d & J \end{array} \right\} \\ &\quad \sum_{Nnn'} I_n I_{n'} M_{n_a l_a n_b l_b}^{NJn_0} M_{n_c l_c n_d l_d}^{NJn'_0} \end{aligned} \quad (47)$$

Collective excitations

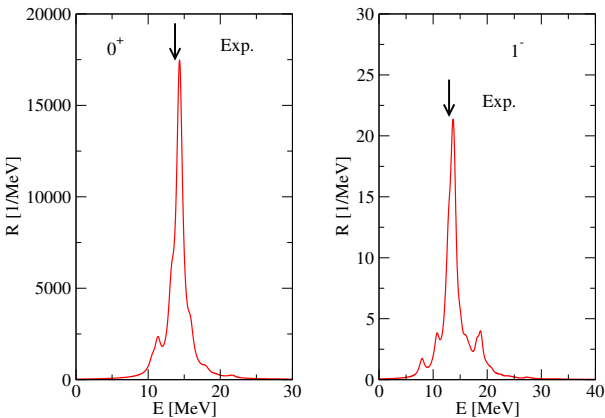


Figure 2: The Isoscalar monopole (left) and isovector dipole (right) strength distribution for ^{208}Pb . ISGMR centroid energy is on 14.2 (exp. 13.96 ± 0.20 MeV, while for RPA IVGDR predicts the excitation energy on 13.7 (exp. 13.3 MeV).

Isoscalar monopole collective excitation

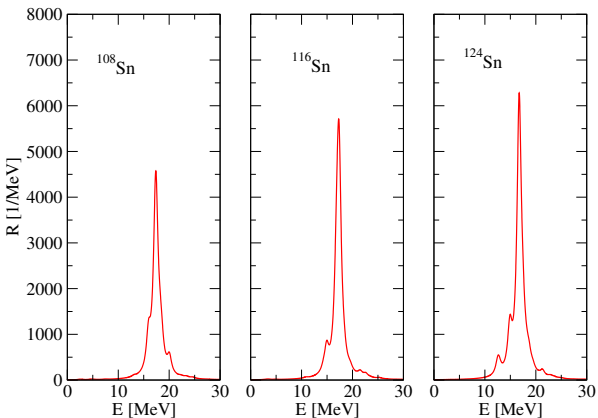


Figure 3: The Isoscalar monopole strength distribution for even-even nuclei $A = 108 - 124$ with $\Delta A = 8$.

Proton-neutron (R)QRPA

RPA equations:

$$\begin{pmatrix} A & B \\ B^* & A^* \end{pmatrix} \begin{pmatrix} X^\lambda \\ Y^\lambda \end{pmatrix} = E_\lambda \begin{pmatrix} 1 & 0 \\ 0 & -1 \end{pmatrix}, \quad (48)$$

$$\begin{aligned} A_{pn,p'n'} &= H_{pp'}^{11} \delta_{nn'} + H_{nn'}^{11} \delta_{pp'} + (u_p v_n u_{p'} v_{n'} + v_p u_n v_{p'} u_{n'}) \\ &\quad \times V_{pn'np'}^{ph} + (u_p u_n u_{p'} u_{n'} + v_p v_n v_{p'} v_{n'}) V_{pnp'n'}^{pp}, \end{aligned} \quad (49)$$

$$\begin{aligned} B_{pn,p'n'} &= (u_p v_n v_{p'} u_{n'} + v_p u_n u_{p'} v_{n'}) V_{pp'nn'}^{ph} \\ &\quad + (u_p u_n v_{p'} v_{n'} + v_p v_n u_{p'} u_{n'}) V_{pnp'n'}^{pp}. \end{aligned} \quad (50)$$

Non-diagonal H^{11} is defined as

$$H^{11} = (u_i u_j + v_i v_j) h_{ij} + (u_i v_j - v_i u_j) \Delta_{ij} \quad (51)$$

Proton-neutron (R)QRPA

Isovector-vector part of PN-(R)QRPA survives only for $V^{(1)}$ type of matrix elements.
 In the case of spacelike components we have:

$$\begin{aligned} V_{abcd}^{(1s)} = & - \int d^3 r_1 \int d^3 r_2 \psi_a^\dagger(\vec{r}_1) (\vec{\tau} \gamma_0 \gamma_\mu)^{(1)} \psi_c(\vec{r}_1) \\ & \times \alpha_{TV}(\rho) \delta(\vec{r}_1 - \vec{r}_2) \psi_b^\dagger(\vec{r}_2) (\vec{\tau} \gamma_0 \gamma^\mu)^{(2)} \psi_d(\vec{r}_2), \quad (52) \end{aligned}$$

and timelike components:

$$\begin{aligned} V_{abcd}^{(1t)} = & \int d^3 r_1 \int d^3 r_2 \psi_a^\dagger(\vec{r}_1) \vec{\tau}^{(1)} \psi_c(\vec{r}_1) \alpha_{TV}(\rho) \\ & \times \delta(\vec{r}_1 - \vec{r}_2) \psi_b^\dagger(\vec{r}_2) \vec{\tau}^{(2)} \psi_d(\vec{r}_2). \quad (53) \end{aligned}$$

Isovector-vector matrix elements

If the radial part of wave function is given by:

$$\psi(r) = \begin{pmatrix} f(r) \\ ig(r) \end{pmatrix} \quad (54)$$

by coupling of angular momentum, we get coupled matrix elements for spacelike part:

$$\begin{aligned} V_{abcd}^{(1s)J} = & 2\hat{J}^{-2} \sum_L \int dr r^2 \alpha_{TV} (f_a(r)g_c(r)\langle j_a || (\sigma_S Y_L)_J || \bar{j}_c \rangle \\ & - g_a(r)f_c(r)\langle \bar{j}_a || (\sigma_S Y_L)_J || j_c \rangle)(f_b(r)g_d(r)\langle \bar{j}_d || (\sigma_S Y_L)_J || j_b \rangle \\ & - g_b(r)f_d(r)\langle j_d || (\sigma_S Y_L)_J || \bar{j}_b \rangle), \end{aligned} \quad (55)$$

and timelike part

$$\begin{aligned} V_{abcd}^{(1t)J} = & 2J^{-2} \int dr r^2 \alpha_{TV} (f_a(r)f_c(r) + g_a(r)g_c(r)) \\ & (f_b(r)f_d(r) + g_b(r)g_d(r)) \langle j_a || Y_J || j_c \rangle \langle j_d || Y_J || j_b \rangle, \end{aligned} \quad (56)$$

Isovector-vector matrix elements

Angular part is given by expressions:

$$\langle j_a || Y_J || j_c \rangle = \frac{1 + (-1)^{l_a + l_c + J}}{2} \frac{\hat{j}_a \hat{j}_c \hat{J}}{\sqrt{4\pi}} (-1)^{j_a - 1/2} \begin{pmatrix} j_a & J & j_c \\ -1/2 & 0 & 1/2 \end{pmatrix}, \quad (57)$$

and

$$\begin{aligned} \langle j_a || (\sigma_S Y_L)_J || j_c \rangle = & \frac{1 + (-1)^{l_a + l_c + J}}{2} \frac{\hat{j}_a \hat{j}_c \hat{J} \hat{L}}{\sqrt{4\pi}} (-1)^{l_a + L} \\ & \times \left[(-1)^{l_c + j_c + 1/2} \begin{pmatrix} 1 & L & J \\ 0 & 0 & 0 \end{pmatrix} \begin{pmatrix} j_a & J & j_c \\ -1/2 & 0 & 1/2 \end{pmatrix} - \right. \\ & \left. \sqrt{2} \begin{pmatrix} 1 & L & J \\ -1 & 0 & 1 \end{pmatrix} \begin{pmatrix} j_a & J & j_c \\ 1/2 & -1 & 1/2 \end{pmatrix} \right]. \quad (58) \end{aligned}$$

Isovector-pseudovector matrix elements

In order to describe the effects of pions in multipolar transitions in PN-RQRPA we use isovector-pseudovector coupling. However, we expect that the strength of pion-nucleon in nuclei coupling should be somewhat reduced by factor of g' :

$$V_{PV} = -g' \left(\frac{f_\pi}{m_\pi} \right)^2 \delta(\vec{r}_1 - \vec{r}_2) (\gamma_0 \gamma_5 \gamma_\mu \vec{\tau})^{(1)} (\gamma_0 \gamma_5 \gamma^\mu \vec{\tau})^{(2)}, \quad (59)$$

where f_π decay constant and m_π mass of pion. The value of g' we don't know *a priori* and should be deduced from experiment.

For timelike part pseudovector matrix elements look like:

$$\begin{aligned} V_{abcd}^{PV(t)J} = & 2g' \hat{J}^{-2} \left(\frac{f_\pi}{m_\pi} \right)^2 \int dr r^2 (f_a(r)g_c(r) - g_a(r)f_c(r)) \\ & \times (f_b(r)g_d(r) - g_b(r)f_d(r)) \langle j_a || Y_J || \bar{j}_c \rangle \langle \bar{j}_d || Y_J || j_c \rangle, \end{aligned} \quad (60)$$

Timelike matrix elements are non-zero only in case of unnatural parity transitions, like Gamow-Teller transition.

Isovector-pseudovector matrix elements

For spacelike part isovector-pseudovector matrix elements look like:

$$\begin{aligned}
 V_{abcd}^{PV(s)J} = & 2g' \hat{J}^{-2} \left(\frac{f_\pi}{m_\pi} \right)^2 \sum_L \int dr r^2 (f_a(r)f_c(r) \\
 & \times \langle j_a | (\sigma_S Y_L)_J | j_c \rangle + g_a(r)g_c(r) \langle \bar{j}_a | (\sigma_S Y_L)_J | \bar{j}_c \rangle) (f_b(r)f_d(r) \\
 & \times \langle j_d | (\sigma_S Y_L)_J | j_b \rangle + g_b(r)g_d(r) \langle \bar{j}_d | (\sigma_S Y_L)_J | \bar{j}_b \rangle). \quad (61)
 \end{aligned}$$

Spacelike isovector-pseudovector matrix elements contribute to both unnatural and natural parity transitions, but in opposite manner compared to isovector-vector matrix elements.

Separable pairing in the case of PN-(R)QRPA

Coupled pp-elements for PN-(R)QRPA are given by:

$$V_{abcd}^{JM} = -G \hat{j}_a \hat{j}_b \hat{j}_c \hat{j}_d \sum_{LS} \left(1 - (-1)^{S+T}\right) \hat{S}^2 \hat{L}^2 \left\{ \begin{array}{ccc} l_b & 1/2 & j_b \\ l_a & 1/2 & j_a \\ L & S & J \end{array} \right\} \left\{ \begin{array}{ccc} l_d & 1/2 & j_d \\ l_c & 1/2 & j_c \\ L & S & J \end{array} \right\} \sum_{nn'} I_n I'_n M_{n_a l_a n_b l_b}^{NLn_0} M_{n_c l_c n_d l_d}^{NLn'_0} \quad (62)$$

This is non-vanishing only for $S = 0$ and $T = 1$ or $S = 1$ and $T = 0$. Assumed form of pp-matrix elements:

$$V_{abcd}^{JM} = \langle ab | V(T=0; S=1) | cd \rangle^{JM} \times V_0 + \langle ab | V(T=1; S=0) | cd \rangle^{JM} \quad (63)$$

We don't know *a priori* the value of factor V_0 . It can be somewhat reduced or enhanced compared to the case $T = 1$.

Determination of parameter g'

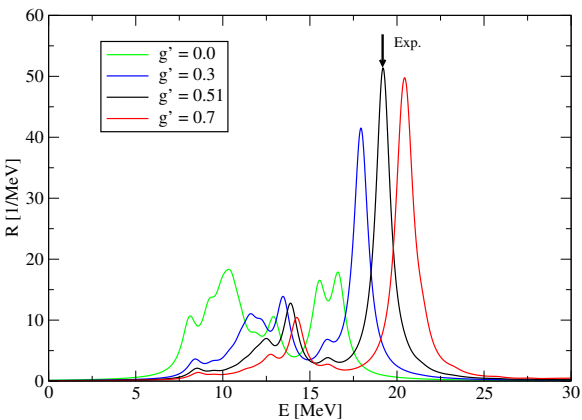


Figure 4: The Gamow-Teller strength distribution for ^{208}Pb for different values of parameter g' , calculated with DD-PC1 interaction. The experimental value of the position of GT^- main peak in ^{208}Pb is on 19.2 MeV. This corresponds to $g' = 0.51$. The width of Lorentzian is 1 MeV.

Gammow-Teller resonance

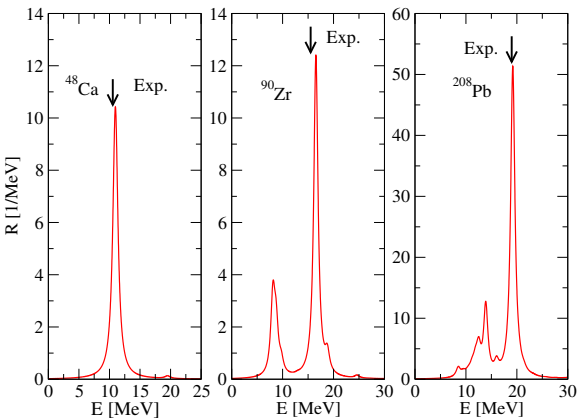


Figure 5: The Gammow-Teller strength distribution for ^{48}Ca ^{90}Zr and ^{208}Pb , calculated by DD-PC1 interaction. The theoretical (experimental) values of central position GTR main peak are 11.0 (10.5) MeV for ^{48}Ca and 16.6 (15.6) MeV for ^{90}Zr .

Isobaric analog resonance

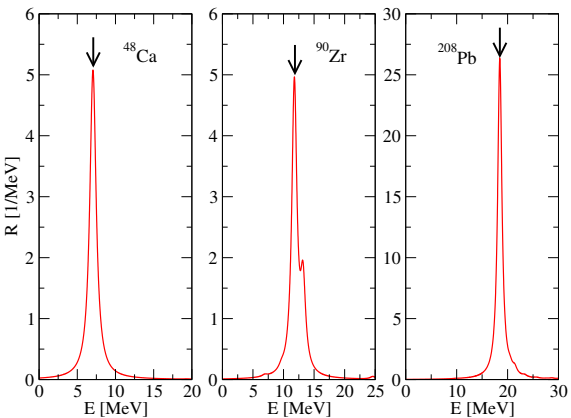


Figure 6: The isobar analog state strength distribution for ^{48}Ca , ^{90}Zr and ^{208}Pb , calculated by DD-PC1. The theoretical (experimental) values of central position GTR main peak are 7.05 (7.17) MeV for ^{48}Ca and 11.7 (11.7 ± 0.9) MeV for ^{90}Zr and 18.47 (18.83 ± 0.02) MeV for ^{208}Pb .

Isobaric analog resonance in Sn isotopes

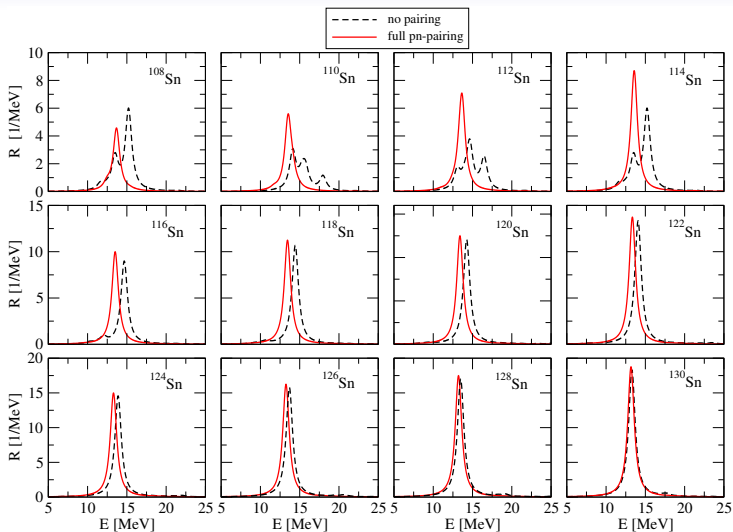


Figure 7: PN-(R)QRPA strength distribution for even-even nuclei with $A = 108 - 130$, calculated by DD-PC1 with separable pairing interaction.

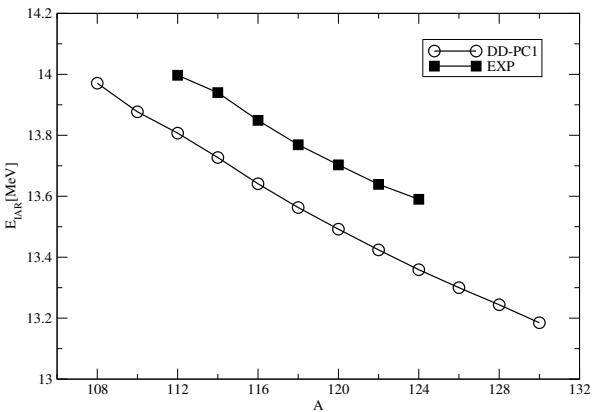


Figure 8: Calculated and experimental IAR position for Sn isotopes.

Gammow-Teller resonance in ^{118}Sn

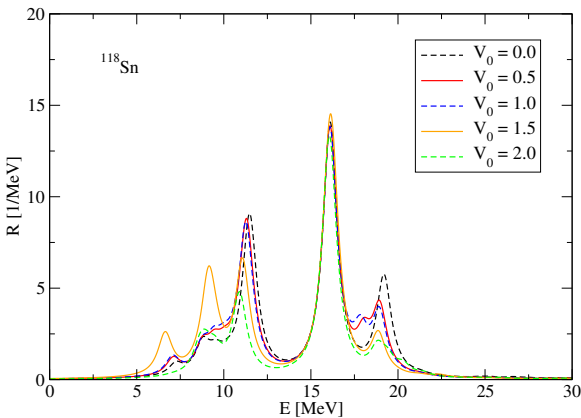


Figure 9: The Gammow-Teller strength distribution for ^{118}Sn for different values of parameter V_0 . Notice, only $T = 0$ pp matrix elements are nonvanishing.

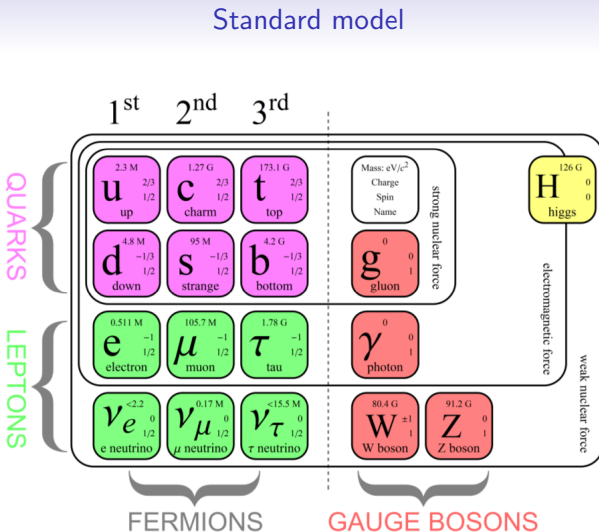


Figure 10: Standard model.

Why neutrino-nucleus reactions?

Neutrino mass hierarchy still remains an open problem due to insensitivity of previous and nowadays experiments on sign of difference between squares of neutrino masses.

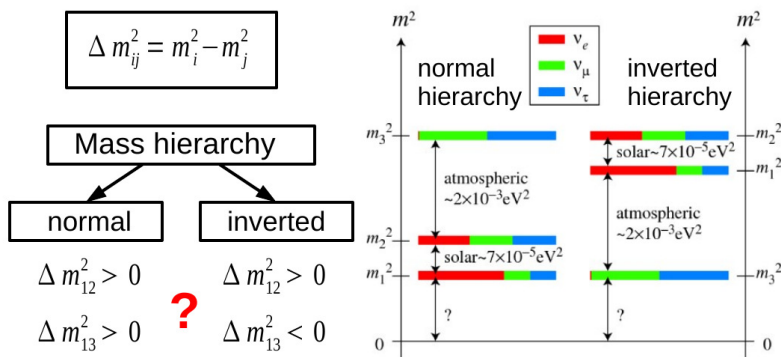


Figure 11: Possible neutrino mass ordering (hierarchy). Degenerate case excluded from figure.

Why neutrino-nucleus reactions?

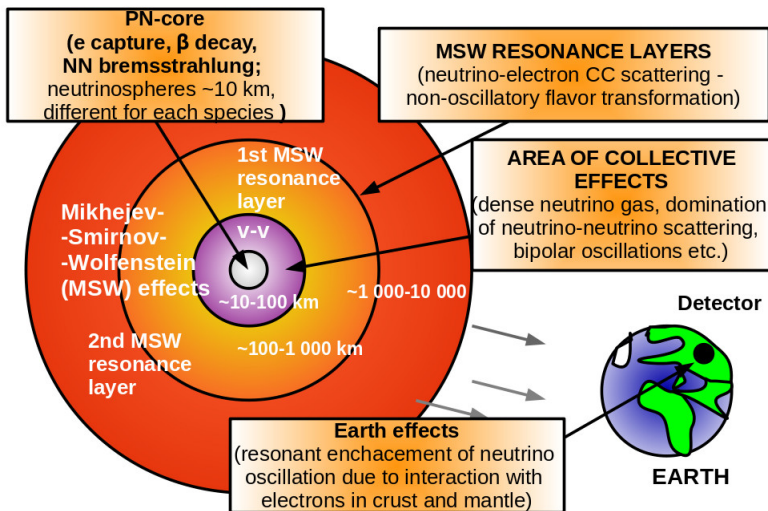


Figure 12: Supernova from neutrino perspective.

Why neutrino-nucleus reactions?

We need to choose adequate target material for detector in order to achieve good statistics and include or exclude particular neutrino species in a specific energy range.

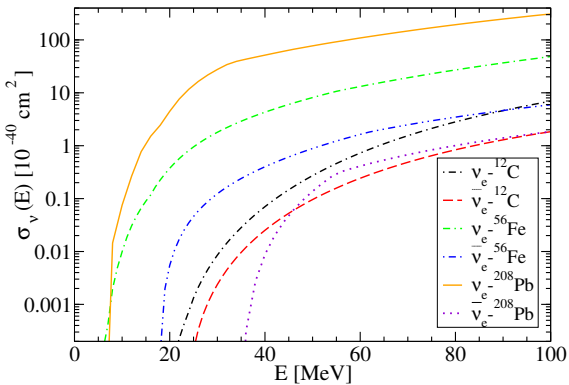


Figure 13: The inclusive $\nu_e(\bar{\nu}_e)$ cross sections with ${}^{12}\text{C}$, ${}^{56}\text{Fe}$ and ${}^{208}\text{Pb}$ as a function of $\nu_e(\bar{\nu}_e)$ energy (charged current reactions only). (see refs. D. Vale, N. Paar AIP Conference Proceedings 1681 (1), 050011; N. Paar, T. Marketin, D. Vale, D. Vretenar International Journal of Modern Physics E 24 (09), 1541004).

Why neutrino-nucleus reactions?

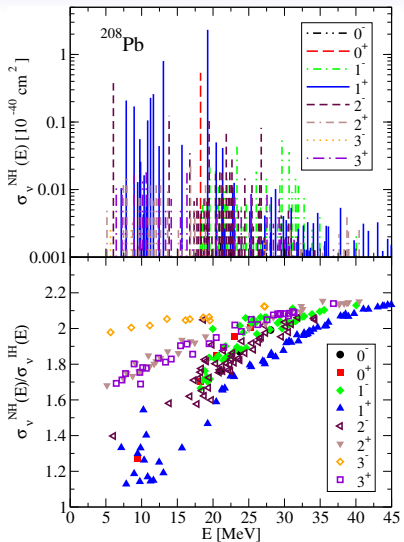


Figure 14: Example of multipole decomposition of the flux averaged cross sections for $\nu_e - {}^{208}\text{Pb}$ charged current reaction. see ref. D Vale, T Rauscher, N Paar Journal of Cosmology and Astroparticle Physics 2016 (02), 007

Why neutrino-nucleus reactions?

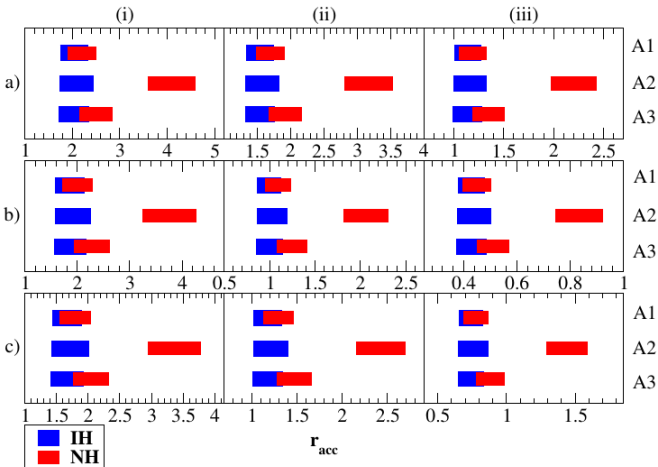


FIG. 6: The ratios r_{acc} of the number of the detector events induced in mineral oil (CH_2), water (H_2O), and ^{208}Pb for the incoming (anti)neutrino fluxes of the accretion phase in normal (NH) and inverted (IH) mass hierarchy: (a) $r_{e^+, \text{in}}^{\text{free p}, \text{Pb}} [10^{-1}]$ (b) $r_{e^+, 2n}^{\text{free p}, \text{Pb}}$ (c) $r_{e^+, \text{tot n}}^{\text{free p}, \text{Pb}} [10^{-1}]$. The three columns correspond to (i) $\langle E_{\nu_e}^0 \rangle = 8 \text{ MeV}$, $\langle E_{\bar{\nu}_e}^0 \rangle = 11 \text{ MeV}$, $\langle E_{\nu_x}^0 \rangle = 13 \text{ MeV}$; (ii) $\langle E_{\nu_e}^0 \rangle = 10 \text{ MeV}$, $\langle E_{\bar{\nu}_e}^0 \rangle = 13 \text{ MeV}$, $\langle E_{\nu_x}^0 \rangle = 15 \text{ MeV}$; and (iii) $\langle E_{\nu_e}^0 \rangle = 12 \text{ MeV}$, $\langle E_{\bar{\nu}_e}^0 \rangle = 15 \text{ MeV}$, $\langle E_{\nu_x}^0 \rangle = 19 \text{ MeV}$. A1, A2, A3 denote the combinations of the luminosity ratios for the accretion phase given in Tab. I.



Why neutrino-nucleus reactions?

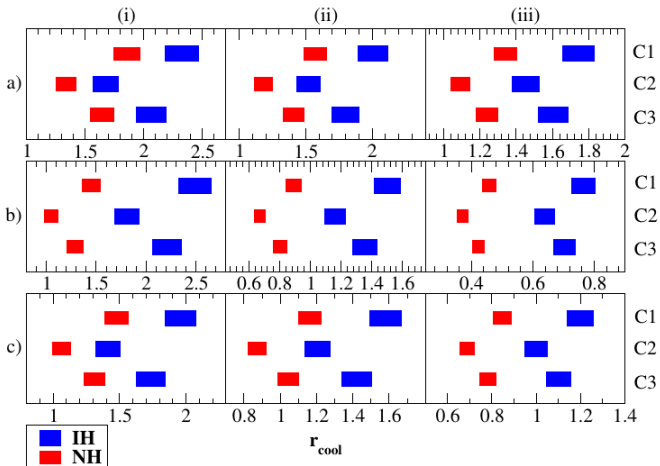


FIG. 7: The ratios r_{cool} of the number of the detector events induced in mineral oil (CH_2), water (H_2O), and ^{208}Pb for the incoming (anti)neutrino fluxes of the cooling phase in normal (NH) and inverted (IH) mass hierarchy for three configurations of initial ν average energies. The same notation as in Fig. 6 applies. C1, C2, C3 denote the combinations of the luminosity ratios for the cooling phase given in Tab. II.